QUANTUM BEATS IN CONTINUOUSLY EXCITED ATOMIC CASCADES

A. ASPECT, J. DALIBARD *, P. GRANGIER and G. ROGER
Institut d'Optique, Université Paris-Sud, F-91406 Orsay, France

Received 5 January 1984

We report on the observation of strong Zeeman beats in the temporal correlation between the two photons emitted in the $4p^2\ ^1S_0 \rightarrow 4s4p\ ^1P_1 \rightarrow 4s^2\ ^1S_0$ cascade in calcium. These beats result from a quantum interference between the various decaying channels. Unlike usual quantum beats, they are observed with a continuous excitation of the upper level.

1. Introduction

When several quantum paths connect two given energy states of a system, it is well known that interferences between these paths may cause "quantum beats" in the evolution of observables of the system [1]. In atomic physics, such a phenomenon has been observed for a long time, for example by sending a resonant laser pulse on an atom with an upper level $|e\rangle$ composed of several non-degenerated sublevels $|e_i\rangle$ [2]. Fluorescence light may then be modulated at Bohr frequencies of $|e_i\rangle$ levels; this results from interferences between the various "absorption-emission" channels through each $|e_i\rangle$. A second possible interpretation of this effect consists in saying that the laser pulse initially prepares the atom in a coherent superposition of $|e_i\rangle$ levels; the evolution of these "coherences" in the following of the process then involves Bohr frequencies of the different $|e_i\rangle$ levels, and this produces the modulation of the fluorescence light.

In this paper, we report the experimental observation of another type of atomic quantum beats, occuring in the emission of two photons in a 3-level atomic cascade $e \rightarrow r \rightarrow g$, where the intermediate state $|r\rangle$ is split into several sublevels $|r_i\rangle$ with different energies (see fig. 1). The various decaying channels from $|e\rangle$ to $|g\rangle$ via different intermediate levels $|r_i\rangle$ interfere and

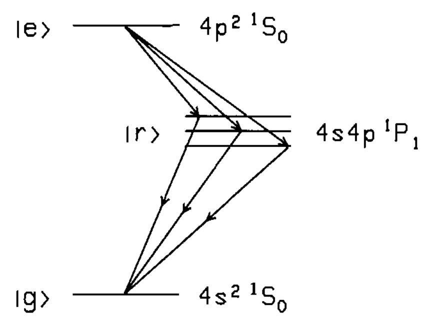

Fig. 1. Interfering decaying channels in an atomic cascade. The indicated level configurations are those of the calcium cascade actually used in our experiment.

this leads to a modulation with τ of the function $P(\nu_1 : t; \nu_2 : t + \tau)$, defined as the joint probability of detecting a photon ν_1 at time t and a photon ν_2 at time $t + \tau$.

A key point of this type of quantum beats lies in the fact that they can be observed with a continuous excitation of the upper level $|e\rangle$. One can say that the first photon detection process prepares the atom in a coherent superposition of levels $|r_i\rangle$ (replacing thus the laser pulse of usual quantum beats).

The subsequent evolution of the atom then involves the Bohr frequencies of the states $|r_i\rangle$, which are reflected in the modulation of the fluorescence ν_2. In this point of view, the comparison between conventional quantum beats and these cascade beats raises some interesting features. In conventional quantum beats experiments, the excitation pulse has to be

* Permanent address: Laboratoire de Physique de l'Ecole Normale Supérieure, F-75231 Paris Cédex 05, France.

0 030-4018/84/$03.00 © Elsevier Science Publishers B.V. (North-Holland Physics Publishing Division)

short enough in order not to wash out the quantum beats. Here, such a problem does not arise since the preparation of the atom in the intermediate levels $|r_i\rangle$, via spontaneous emission of photon ν_1, can be considered as a percussional process (more precisely, the analogous of the laser pulse duration is the inverse of the bandwidth of the frequency filter selecting photon ν_1, i.e. less than 10^{-13} s). Also, in usual quantum beats, one selects the excited coherences by a choice of the polarization of the laser pulse. Here, a similar role is played by the choice of the polarization for the detection of the first photon ν_1.

Although they have been predicted long ago [3], there are a very small number of experimental observations of such effect [4] ‡1. For the experiments that we know in atomic physics [4], the observed beats had a visibility much smaller than the value theoretically achievable, mainly because of weak signals implying hundreds of hours of data accumulations.

In the experiment reported in this paper, we have used a very efficient continuous source of pairs of photons emitted in a $J = 0 \rightarrow J = 1 \rightarrow J = 0$ cascade in calcium (see fig. 1), giving a time delayed coincidence spectrum (i.e.: $P(\nu_1, t : \nu_2, t + \tau)$ averaged on t), with a good signal-to-noise ratio, in a few minutes. We have observed good visibility quantum beats, when the Zeeman sublevels of the $J = 1$ intermediate state are separated by an external magnetic field. The signal-to-noise ratio was good enough to allow an accurate comparison with the theoretical predictions, for various configurations of the magnetic field and of detecting polarizations. A Q.E.D. calculation of the observed beats is given in the appendix.

2. Experimental set-up

The upper $4p^2\ {}^1S_0$ level in calcium is populated by continuous two-photon excitation, from a single-line krypton ion laser ($\lambda_K = 406$ nm) and a tunable Rh 6G dye laser ($\lambda_D = 581$ nm). The two lasers are focused on a calcium atomic beam, the interaction region being roughly a cylinder 0.5 mm long and 70 μm in diameter. A typical density in the atomic beam is 2×10^{10} atoms/cm^3, low enough to prevent any significant radiation trapping or Faraday effect in our experimental conditions. The rate of emission of the cascade ($\lambda_1 = 551$ nm, $\lambda_2 = 422$ nm) is about $2 \times 10^7\ \mathrm{s}^{-1}$. The efficiency of each detection channel is over 10^{-3}, yielding counting rates of more than $20\,000\ \mathrm{s}^{-1}$. This source was previously described with more details in ref. [6]. The magnetic field, created by two coils inside the vacuum chamber, can be varied up to 100 Gauss. Its stability and homogeneity over the interaction region, are better than 0.5%, taking into account the effect of the earth magnetic field.

The source is in view of two detection channels, respectively selecting photons ν_1 and ν_2 with use of interference filters. The bandwidth of each filter (2 nm FWHM) is much greater than the Zeeman splittings (less than 10^{-4} nm). On each detection channel, a multidielectric coating polarizer can be set, separating the two orthogonal linear polarizations with good efficiency [7]. Each polarizer is followed by two photomultipliers, feeding a fourfold coincidence system, that involves a time to amplitude converter and a multichannel analyser. The width of a channel is 0.41 ns, while the response of the whole electronics is well represented by a gaussian curve 1.2 ns HWHM; this value is mainly due to the dispersion of transit times in the photomultipliers.

3. Results and interpretations

A typical experimental result is sketched on fig. 2; it has been obtained with the configuration represented on fig. 3, corresponding to a magnetic field $\boldsymbol{B} = B\boldsymbol{e}_z$ perpendicular to the detection channel axis $\boldsymbol{e}_x$. Polarization measurements on ν_1 and ν_2 photons are performed along $\boldsymbol{e}_y$ or $\boldsymbol{e}_z$, and we have displayed on fig. 2 the four corresponding time-delayed coincidence spectra. The first spectrum (both polarization measurements along $\boldsymbol{e}_y$) exhibits a clear modulation with a period 6 ns, superimposed on the exponential decay of the intermediate state of the cascade (lifetime 5 ns).

All these results can be easily understood using the picture given in the introduction: the detection of the first photon ν_1 prepares the atom in a coherent superposition of the Zeeman sublevels $|r; m = 0, \pm 1\rangle$, which then evolves in the magnetic field. When the first

‡1 Such beats have also been observed in nuclear γ cascades. See for example ref. [5].

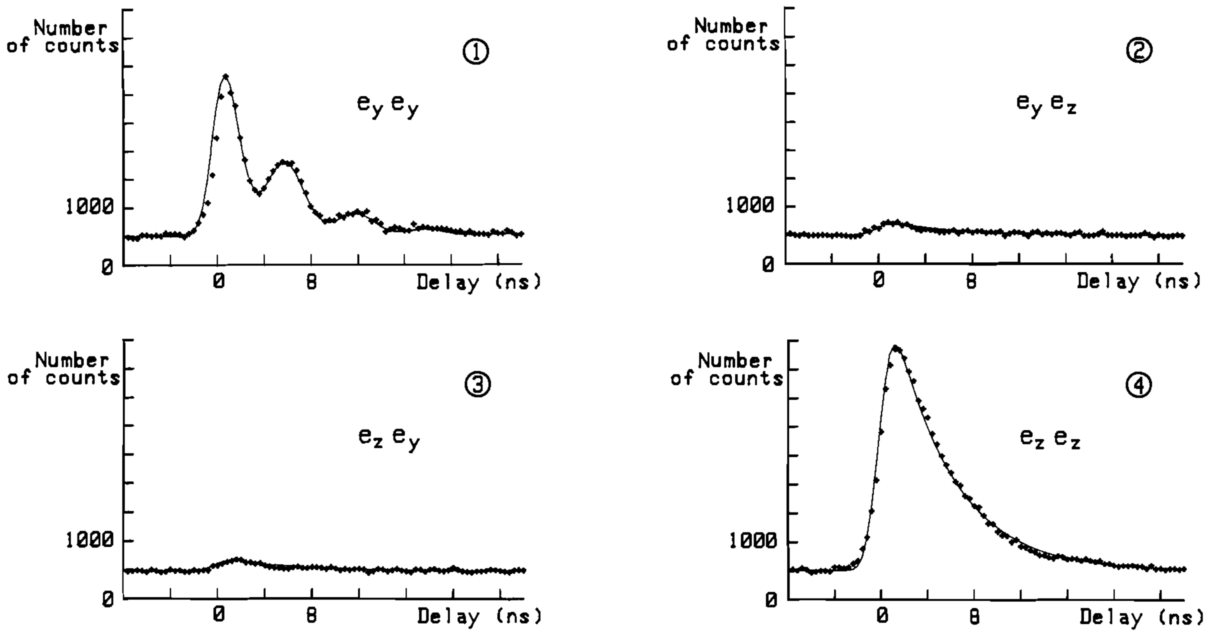

Fig. 2. Time delayed coincidence spectra between ν_1 and ν_2, in the four polarization configurations of fig. 3. The background of accidental coincidences is 500 counts per channel, and the peak number of counts is 4000. The full lines are theoretical fits corresponding to $g_J = 1$.

photon is detected with a polarization along e_y (σ polarization), the subsequent atomic state is $1/\sqrt{2}$ $(|r; m = +1\rangle + |r; m = -1\rangle)$, describing a dipole aligned along e_y. This dipole then precesses around B (e_z axis) at the Larmor frequency. The light emitted in the direction e_x (ν_2 photon) is thus polarized along e_y and modulated at the Larmor frequency. This explains the two first spectra of fig. 2. The two last spectra correspond to a photon ν_1 detected with a polarization along e_z (π polarization), and the intermediate atomic state is now $|r; m = 0\rangle$. This state (describing a dipole aligned along e_z) does not evolve in the magnetic field, so that the light emitted (ν_2 photon) is polarized along e_z and is not modulated.

One can also render an account for these experimental results using the point of view of interfering quantum paths. For ν_1 and ν_2 fluorescence photons polarized along e_y (σ polarization), two desexcitation routes, via Zeeman sublevels $|r; m = +1\rangle$ and $|r; m = -1\rangle$; have to be considered, and the amplitudes associated with these routes interfere leading to the modulation observed on the first spectrum. For ν_1 and

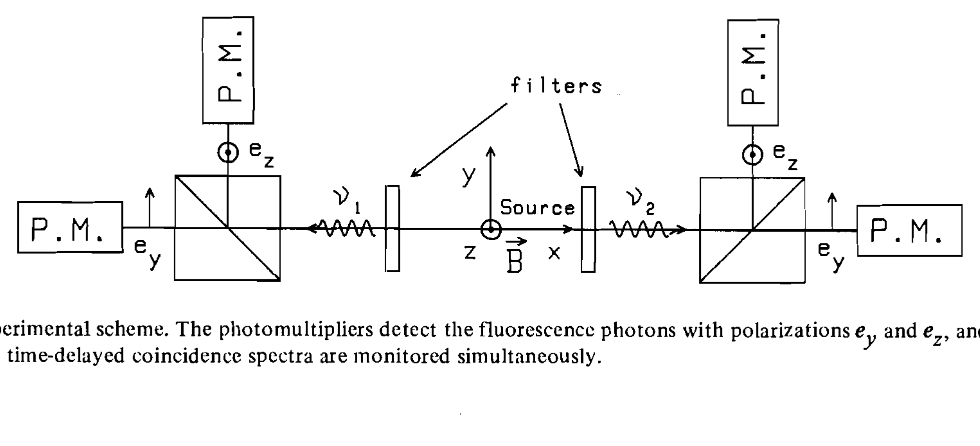

Fig. 3. Experimental scheme. The photomultipliers detect the fluorescence photons with polarizations e_y and e_z, and the four corresponding time-delayed coincidence spectra are monitored simultaneously.

ν_2 fluorescence photons polarized along $\boldsymbol{e}_z$ (π polarization), there is only one relevant desexcitation channel (via $|r; m = 0\rangle$) and no modulation can be observed (fourth spectrum). On the other hand, there is obviously no path allowing emission of "σ polarized" ν_1 photon and a "π polarized" ν_2 photon (or vice-versa) and this explains the quite flat second and third spectra.

An explicit calculation of correlation signals has been performed in this second point of view, and is outlined in the appendix (section 5). Results are found in complete agreement with the qualitative predictions given above. This calculation allows to take into account the finite aperture of the detecting lenses and the efficiencies of the polarizers; that accounts for a decrease of the visibility of the modulation and for a residual hunch appearing on the spectra 2 and 3. At last, we have convoluated the theoretical expression with a gaussian curve associated to the finite response time of electronics. Treating the modulation frequency as an adjustable parameter, we have been able to obtain an excellent fit to the experimental data (see fig. 2). We have measured in this way the Larmor frequency as a function of the magnetic field, and we have finally determined the Landé factor of the intermediate level $|r\rangle$:

$$g_J = 1.00 \pm 0.01 .$$

This value is consistent with the expected value $g_J = 1$ value for the 4s 4p $^1P_1$ level and in agreement with other measurements [8] [‡2].

Let us finally mention that we have studied other experimental configurations. Another particularly interesting case corresponds to a magnetic field aligned with the detection channel axis (see appendix). Here also, experimental and theoretical results have been found in complete agreement.

4. Concluding remarks

As we already emphasized it, the observed beats are a typical quantum interference effect. In particular, the difference between the first and fourth spectra of fig. 2 illustrates the general rule that any attempt to determine through which path the process has occured results in the disappearance of the beat pattern.

In close relation with this remark, we can notice that there is no hope to observe beats on the singles counting rate in a $J = 0 \to J = 1 \to J = 0$ cascade, even with a pulsed excitation of the upper level. For instance, one cannot observe a modulation of the intensity of the fluorescence light ν_2, resulting from an interference between different desexcitation routes. As a matter of fact, it would still be possible, at least in a "Gedankenexperiment", to determine later on, by a suitable measurement of polarization and/or energy of photon ν_1, which path was followed in the desexcitation process [‡3].

That the interferences (i.e. beats) can be observed on correlation signals is understandable by noticing that our experiments involve a measurement on ν_1, that "erases" the "which path" information. In this respect, our situation thus appears closely related to the so-called "quantum eraser" gedankenexperiments [11].

5. Appendix

We outline in this appendix a Q.E.D. analysis of the observed quantum beats, based on the scattering theory. A "precollision" ket $|\psi_i\rangle$ describes the atom in its ground state, in presence of two incident laser wave packets, which are assumed to contain N' photons in the mode $(\boldsymbol{k}', \boldsymbol{\varepsilon}')$ and N'' photons in the mode $(\boldsymbol{k}'', \boldsymbol{\varepsilon}'')$; we have therefore

$$|\psi_i\rangle = |g, N'\lambda', N''\lambda''\rangle ,$$

where λ', λ'' stand for the impulsions $\boldsymbol{k}'$, $\boldsymbol{k}''$ and the polarizations $\boldsymbol{\varepsilon}'$, $\boldsymbol{\varepsilon}''$ of the two laser modes.

The "post collision" ket $|\psi_i\rangle$ will be expanded up to the second order in the laser–atom interaction, assuming that the excitation rate is weak. At this order, $|\psi_f\rangle$ appears as the sum of three terms. The first one

‡2 Let us notice that this measurement was made using conventional quantum beats.

‡3 This argument, confirmed by the calculations relative to quantum beats in cascades excited by pulsed lasers, may not hold for more complex strucures of the levels, as shown by recent experimental [9] and theoretical works [10]. Intensity beats can actually be observed in cascades, if some definite conditions on the level structures are fulfilled. One can easily check that these conditions amount to the impossibility of determining the followed desexcitation channel, by any measurement on photon ν_1. These conditions cannot be fulfilled in our $J_e = 0$ case.

is simply the incident wave packet $|\psi_i\rangle$, the second one corresponds to elastic scattering of laser photons (Rayleigh diffusion) and the third one is due to inelastic scattering. Since filters eliminate the lasers frequencies, our calculation will be restricted to the evaluation of this third term:

$$|\psi_{f\,\mathrm{inel}}^{(2)}\rangle = \sum_{\lambda_a,\lambda_b} S_2(\lambda_a,\lambda_b)$$

$$\times\; |g, (N'-1)\lambda', (N''-1)\lambda'', \lambda_a, \lambda_b\rangle,$$

where $S_2(\lambda_a, \lambda_b)$ is the second order matrix element of the S matrix, corresponding to the scattering of two laser photons from the modes λ', λ'' to the modes $(\boldsymbol{k}_a, \boldsymbol{\varepsilon}_a)$, $(\boldsymbol{k}_b, \boldsymbol{\varepsilon}_b)$ denoted by λ_a and λ_b.

The amplitude $S_2(\lambda_a, \lambda_b)$ can be calculated in formal collision theory as the sum of diagrams involving the same initial and final states of the atom. One diagram is represented on fig. 4; 36 such diagrams are involved in the scattering process, obtained by permutations of λ' and λ'', λ_a and λ_b, for all possible intermediate levels $|r, m\rangle$ and $|r, m'\rangle$ ($m = 0, \pm 1$ and $m' = 0, \pm 1$).

The contribution of one diagram involves matrix elements of the laser–atom interaction, associated with each vertex, and energy denominators associated with the intermediate states of the atom plus field system.

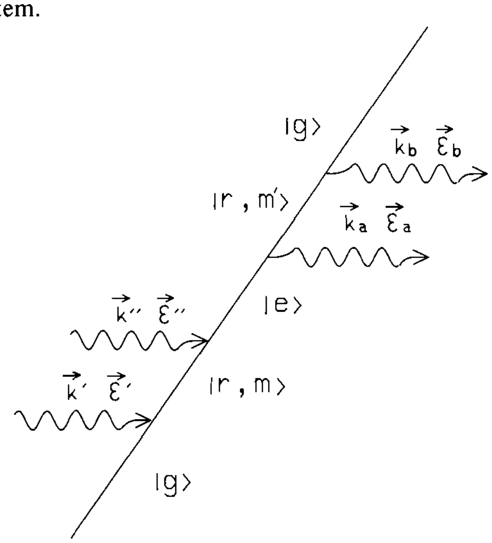

Fig. 4. Diagram of an inelastic second order scattering process. Two photons are scattered from the modes $\lambda'(\boldsymbol{k}', \boldsymbol{\varepsilon}')$, $\lambda''(\boldsymbol{k}'', \boldsymbol{\varepsilon}'')$ to the modes $\lambda_a(\boldsymbol{k}_a, \boldsymbol{\varepsilon}_a)$ and $\lambda_b(\boldsymbol{k}_b, \boldsymbol{\varepsilon}_b)$. The intermediate atomic states are the upper level $|e\rangle$ and the Zeeman sublevels $|r, m\rangle$ or $|r, m'\rangle$.

We shall not give explicit expressions of these diagrams, which are close to those calculated in refs. [12] and [13]. After complete calculation, $S_2(\lambda_a, \lambda_b)$ appears to factorize in two parts, due to the non-degeneracy of level $|e\rangle$: the first part corresponds to the two-photon laser excitation of $|e\rangle$, and the second one, which interests us here, corresponds to the desexcitation of $|e\rangle$ to $|g\rangle$ via $|r, m\rangle$.

From Glauber's formalism [14], the joint density of probability for detecting a photon of polarization $\boldsymbol{\varepsilon}_A$ at point $\boldsymbol{r}_A$ and time t_A and a photon of polarization $\boldsymbol{\varepsilon}_B$ at point $\boldsymbol{r}_B$ and time t_B is

$$w_{AB}(\boldsymbol{r}_A, t_A, \boldsymbol{r}_B, t_B)$$

$$= C\langle\psi_f|E_A^-(\boldsymbol{r}_A, t_A)E_B^-(\boldsymbol{r}_B, t_B)E_B^+(\boldsymbol{r}_B, t_B)E_A^+(\boldsymbol{r}_A, t_A)|\psi_f\rangle.$$

C is some multiplicative constant and $E_A^-(\boldsymbol{r}, t)$, $E_A^+(\boldsymbol{r}, t)$ (resp. E_B^-, E_B^+) are the $\boldsymbol{\varepsilon}_A$ (resp. $\boldsymbol{\varepsilon}_B$) polarization component of the negative and positive frequency parts of the electric field operator, filtered at frequency ω_A (resp. ω_B), and taken in the Heisenberg point of view:

$$E_A^+(\boldsymbol{r}, t) = \mathrm{i}\sum_{\boldsymbol{k}, \boldsymbol{\varepsilon}} \mathcal{E}(\omega)\boldsymbol{\varepsilon}_A\cdot\boldsymbol{\varepsilon}$$

$$\times\; g_A(\omega)\exp[\mathrm{i}(\boldsymbol{k}\cdot\boldsymbol{r} - \omega t)]\, a_{\boldsymbol{k},\boldsymbol{\varepsilon}},$$

where $g_A(\omega)$ resp. $g_B(\omega)$ is a filtering function at frequency $\omega_A \approx \omega_1$ (resp. $\omega_B \approx \omega_2$). $\mathcal{E}(\omega)$ insures that $a_{\boldsymbol{k},\boldsymbol{\varepsilon}}$ is dimensionless. It is then easy to show that

$$w_{AB} = C|\alpha_{AB}|^2,$$

where

$$\alpha_{AB} = \sum_{\lambda_a\lambda_b} S_2(\lambda_a, \lambda_b)\mathcal{E}(\omega_a)\mathcal{E}(\omega_b)$$

$$\times\; g_A(\omega_a)g_B(\omega_b)(\boldsymbol{\varepsilon}_a\cdot\boldsymbol{\varepsilon}_A)(\boldsymbol{\varepsilon}_b\cdot\boldsymbol{\varepsilon}_B)$$

$$\times\; \exp[\mathrm{i}(\boldsymbol{k}_a\cdot\boldsymbol{r}_A - \omega_a t_A)]\exp[\mathrm{i}(\boldsymbol{k}\cdot\boldsymbol{r}_B - \omega_b t_B)]$$

In order to perform the integration over λ_a and λ_b, we suppose that the scattering atom is at $\boldsymbol{r} = \boldsymbol{0}$, and that the detectors subtend small solid angles around the directions $\boldsymbol{r}_A$ and $\boldsymbol{r}_B$; we have then

$$\omega_a t_A - \boldsymbol{k}_a\cdot\boldsymbol{r}_A = \omega_a(t_A - r_A/c) = \omega_a\tau_A,$$

$$\omega_b t_B - \boldsymbol{k}_b\cdot\boldsymbol{r}_B = \omega_b(t_B - r_B/c) = \omega_b\tau_B,$$

and we define $\tau = \tau_B - \tau_A$.

Omitting a multiplicative constant (that includes the excitation process) the integration over λ_a and λ_b yields

$$\alpha_{AB} = \left(\sum_{m=0,\pm 1} \langle e|\boldsymbol{D} \cdot \boldsymbol{\varepsilon}_A^*|r, m\rangle\langle r, m|\boldsymbol{D} \cdot \boldsymbol{\varepsilon}_B^*|g\rangle e^{-im\omega\tau} \right)$$

$$\times \exp(-i\omega_1 \tau_A) \exp(-i\omega_2 \tau_B) H(\tau) \exp(-\Gamma\tau/2),$$

where $\hbar\omega$ and Γ are the Zeeman splitting and the natural width of the r level, $\boldsymbol{D}$ the dipole operator, and $H(\tau)$ the Heaviside function.

The expression of α_{AB} shows clearly that the interference between the three "paths" $|e\rangle \to |r, m\rangle \to |g\rangle$ ($m = 0, \pm 1$) is responsible for the observed quantum beats.

The matrix element of the dipole operator can be rewritten using Wigner-Eckart theorem, and we obtain eventually, omitting the multiplicative constant

$$\omega_{AB} = |(\epsilon_{x_A}\epsilon_{x_B} + \epsilon_{y_A}\epsilon_{y_B}) \cos \omega\tau$$

$$+ (\epsilon_{x_A}\epsilon_{y_B} - \epsilon_{y_A}\epsilon_{x_B}) \sin \omega\tau$$

$$+ \epsilon_{z_A}\epsilon_{z_B}|^2 H(\tau) \exp(-\Gamma\tau)$$

where the axes are defined so that the magnetic field is along Oz (quantization axis).

Let us consider now some simple marginal values of this expression. For the experimental configuration of fig. 3, with the detection channel axis along $\boldsymbol{e}_x$, one obtains for the two possible polarizations $\boldsymbol{e}_y$ and $\boldsymbol{e}_z$

$$w_{e_y e_y} = (\tfrac{1}{2} + \tfrac{1}{2} \cos 2\omega\tau) H(\tau) \exp(-\Gamma\tau),$$

$$w_{e_y e_z} = \omega_{e_z e_y} = 0, \quad w_{e_z e_z} = H(\tau) \exp(-\Gamma\tau).$$

These results confirms the qualitative predictions of section 3.

In another simple case, the detectors and the source would be aligned along the z-axis (direction of $\boldsymbol{B}$), the orientations of the polarizers being defined by the azimuthal angles ϕ_A and ϕ_B (between $\boldsymbol{e}_x$ and $\boldsymbol{\varepsilon}_A$ or $\boldsymbol{\varepsilon}_B$). We obtain then

$$w_{\phi_A \phi_B} = \cos^2(\omega\tau - (\phi_A - \phi_B)) H(z) \exp(-\Gamma\tau).$$

We have thus beats, the phase of which depends on the relative angle of the polarizers. The reader can easily convince himself that a picture similar to the one of section 3 is also very clear in this case.

Let us finally notice that, in order to get a quantitative agreement with the experimental data, we take into account the finite aperture of the lenses (summation over the directions $\boldsymbol{r}_A$, $\boldsymbol{r}_B$), and the efficiencies of the polarizers; this results in a predicted small hunch for $w_{e_y e_z}$ and $w_{e_z e_y}$, and in a slight decrease of the visibility of the beats; actually, the previous expression of $w_{e_y e_y}$ is replaced by

$$w_{e_y e_y} = (a + b \cos 2\omega\tau) H(\tau) \exp(-\Gamma\tau),$$

with

$$(b/a)_{yy} = 0.73.$$

References

[1] G. Breit, Rev. Mod. Phys. 5 (1933) 91.

[2] S. Haroche, Topics in applied physics, ed. K. Shimoda (Springer-Verlag Berlin, 1976) p. 253.

[3] M.I. Podgoretskii and O.A. Khrustalev, Sov. Phys. Usp. 6 (1964) 682.

[4] A.M. Dumont, C. Camhy-Val, M. Dreux and R. Vitry, C.R. Acad. Sci. 271 B (1970) 1021;
M. Popp, C. Schäfer and E. Bodenstedt, Z. Phys. 240 (1970) 71;
M.K. Simmons, Ph.D. thesis, Berkeley (1972), unpublished.

[5] R.M. Steffen and H. Frauenfelder, in: Perturbed angular correlations, Vol. 2, eds. E. Karlsson, E. Mathias and K. Siegbahn (North-Holland, Amsterdam, 1964) p. 997.

[6] A. Aspect, P. Grangier and G. Roger, Phys. Rev. Lett. 47 (1981) 460.

[7] A. Aspect, P. Grangier and G. Roger, Phys. Rev. Lett. 49 (1982) 91.

[8] P. Schenk, R.C. Hilborn, H. Metcalf, Phys. Rev. Lett. 31 (1973) 189.

[9] B.J. Dalton, D.S. Gough, P. Hannaford and R.M. Lowe, J. Phys. B; At. Mol. Phys. 15 (1982) L 515.

[10] R. Luypaert and J. Van Craen, J. Phys. B: Atom. Mol. Phys. 12 (1979) 2613;
B.J. Dalton, J. Phys. B: Atom. Molec. Phys. 12 (1979) 2625.

[11] M.O. Scully and K. Drühl, Phys. Rev. A 25 (1982) 2208;
A.G. Zajonc, Phys. Lett. 96 A (1983) 61.

[12] A. Aspect, Thèse, Orsay no. 2674 (1983) (unpublished).

[13] J. Dalibard and S. Reynaud, J. Physique 44 (1983) 1337.

[14] R.J. Glauber, Ecole d'Eté des Houches 1964, in: Quantum optics and electronics, eds. C. de Witt, A. Blandin and C. Cohen-Tannoudji (Gordon and Breach, 1965) p. 63.